Nifuroxazide induces the apoptosis of human non-small cell lung cancer cells through the endoplasmic reticulum stress PERK signaling pathway

DELIANG LI[1,2*], LIPING LIU[1*], FENG LI[3], CHENGSHAN MA[4] and KELI GE[5]

[1]The First Clinical Medical College, Medicine College, Qingdao University, Qingdao, Shandong 266023; [2]Emergency Department, Affiliated Hospital of Qingdao University, Qingdao, Shandong 266000; [3]Traditional Chinese Medicine Department, Zibo Wanjie Cancer Hospital, Zibo, Shandong 255200; [4]Orthopedic SurgeryDepartment, Shandong Provincial Hospital Affiliated to Shandong First Medical University, Jinan, Shandong 250000; [5]School of Basic Medicine, Medical College, Qingdao University, Qingdao, Shandong 266023, P.R. China

Received September 14, 2022; Accepted January 26, 2023

DOI: 10.3892/ol.2023.13834

Abstract. The aim of the present study was to investigate the molecular mechanism of nifuroxazide (NFZ) in the induction of apoptosis of NCI-H1299 human non-small cell lung cancer (NSCLC) cells through the reactive oxygen species (ROS)/Ca^{2+}/protein kinase R-like ER kinase (PERK)-activating transcription factor 4 (ATF4)-DNA damage inducible transcript 3 (CHOP) signaling pathway. Morphological changes of cells were observed by microscopy, and the apoptosis and intracellular ROS levels of cells were observed by inverted fluorescence microscopy. Cell viability after the addition of the PERK inhibitor, GSK2606414, were detected by Cell Counting Kit-8 assay. Annexin V-FITC was used to detect cell apoptosis, Brite 670 was used to detect intracellular ROS and Fura Red AM was used to detect Ca^{2+} content. Western blotting was used to detect PERK, phosphorylated (P)-PERK, ATF4, CHOP, P-Janus kinase 2 and P-signal transducer and activator of transcription 3 expression levels. Compared with the dimethyl sulfoxide control group, NFZ inhibited the survival activity in the H1299 NSCLC cell line, in a time- and dose-dependent manner. However, GSK2606414 inhibited the NFZ-induced apoptosis of H1299 cells. GSK2606414 also inhibited the increase in ROS and Ca^{2+} in H1299 cells induced by NFZ. Western blotting results demonstrated that NFZ significantly increased the expression levels of P-PERK, ATF4 and CHOP, whereas GSK2606414 significantly reduced the NFZ-induced increase in these protein expression levels. In conclusion, NFZ may induce the apoptosis of H1299 NSCLC cells through the ROS/Ca^{2+}/PERK-ATF4-CHOP signaling pathway.

Introduction

With the increasing incidence and mortality rates, cancer remains a primary public health problem. According to the GLOBOCAN 2020 global cancer analysis, the incidence of lung cancer ranks second in the world, with >2.2 million cases (11.4%) and >1.79 million deaths (18%) every year (1). Non-small cell lung cancer (NSCLC) accounts for 80-85% of cases of lung cancer (2,3). In recent years, EGFR-tyrosine kinase inhibitors (TKIs) have played a role in molecular targeted therapy of NSCLC, improving the prognosis of patients with NSCLC. Treatment with TKIs has revolutionized the overall survival time and quality of life in patients with NSCLC with EGFR mutations (4). The use of TKIs in NSCLC depends on the presence of EGFR mutations (5). Although EGFR plays an important role in the occurrence and development of lung cancer, patients with lung cancer with EGFR gene mutations account for 25% of NSCLC cases and are prone to drug resistance and high cytotoxicity (6). It is an urgent problem to find an effective anti-lung cancer drug with low toxicity; however, the elaboration of new mechanisms of action of drugs already in clinical application, or the study of new derivatives of drugs with low toxicity, can save the time and cost of drug development (7).

Correspondence to: Dr Keli Ge, School of Basic Medicine, Medical College, Qingdao University, 38 Dengzhou Road, Qingdao, Shandong 266023, P.R. China
E-mail: ntfadu@163.com

Dr Chengshan Ma, Orthopedic Surgery Department, Shandong Provincial Hospital Affiliated to Shandong First Medical University, 9677 Jingshi Road, Lixia, Jinan, Shandong 250000, P.R. China
E-mail: ma_c_sh@hotmail.com

*Contributed equally

Abbreviations: NFZ, nifuroxazide; ERS, endoplasmic reticulum stress; PERK, protein kinase R-like ER kinase; ATF4, activating transcription factor 4; CHOP, DNA damage inducible transcript 3; DMSO, dimethyl sulfoxide; ROS, reactive oxygen species; JAK2, Janus kinase 2; STAT3, signal transducer and activator of transcription 3

Key words: NFZ, PERK, ATF4, CHOP, NCI-H1299, ERS

The discovery of the therapeutic potential of nitrofuran derivatives dates back to 1948 when it was discovered how they induced antimicrobial activity (8). Nifuroxazide (NFZ), a gastrointestinal antibiotic, was first patented in 1961 (England), 1966 (France) and 1966 (USA) by Robert & Carrie Laboratories (9). In previous years, it has been mainly used to prevent bacillary dysentery and enteritis (10). Previous studies have also shown that NFZ has anti-inflammatory, anti-infection, anti-diabetes, anti-renal fibrosis, anti-pulmonary fibrosis and antiproliferative activity, and ameliorates the lipid and glucose metabolism of HepG2 liver cancer cells (11-15).

The role of NFZS in small cell lung cancer is unclear. The purpose of the present study was to investigate the relationship between NFZ and H299 cell apoptosis, reactive oxygen species (ROS) and ER stress (ERS), and to explore whether NFZ is a PERK mechanism through one of the classical pathways of ERS.

Materials and methods

Materials and instruments. Human NSCLC cells, NCI-H1299 (National Infrastructure of Cell Line Resource), were cultured in DMEM high glucose medium (Hyclone; Cytiva) containing 10% fetal bovine serum (Gibco; Thermo Fisher Scientific, Inc.) in a cell incubator at 37˚C and 5% CO_2.

NFZ and GSK2606414 were purchased from Selleck Chemicals. With dimethyl sulfoxide (DMSO) as the solvent, they were prepared into 50 mM storage solutions and stored at -80˚C. The following reagents were also used in the present study: Antibodies against protein kinase R-like ER kinase (PERK; 1:1,000; #5683; CST Biological Reagents Co., Ltd.), P-PERK (1:1,000; #3179; CST Biological Reagents Co., Ltd.), activating transcription factor 4 (ATF4; 1:1,000; #11815; CST Biological Reagents Co., Ltd.), DNA damage inducible transcript 3 (CHOP; 1:1,000; #2895; CST Biological Reagents Co., Ltd.), Janus kinase 2 (JAK2; 1:1,000; #3230; CST Biological Reagents Co., Ltd.), P-JAK2 (1:1,000; #3771; CST Biological Reagents Co., Ltd.), signal transducer and activator of transcription 3 (STAT3; 1:1,000; #9139; CST Biological Reagents Co., Ltd.), P-STAT3 (1:1,000; #9145; CST Biological Reagents Co., Ltd.), HRP-linked Anti-Rabbit IgG (1:5,000; #7074; CST Biological Reagents Co., Ltd.), HRP-linked Anti-Mouse IgG (1:5,000; #7076; CST Biological Reagents Co., Ltd.), HRP-conjugated β-actin (1:5,000; #4967; CST Biological Reagents Co., Ltd.) and HRP-conjugated GAPDH (1:5,000; #3683; CST Biological Reagents Co., Ltd.); Annexin V/PI kit and BCA kit (both from Yeasen Biotechnology Co., Ltd.); Brite 670 (AmyJet Scientific, Inc.) and Fura Red AM (A&D Technology); DAPI (Sigma-Aldrich; Merck KgaA).

The following instruments were used in the present study: BB15 CO_2 incubator (Thermo Fisher Scientific, Inc.), desktop low-temperature 5810R centrifuge, BD Accuri™ C6 flow cytometer (BD Biosciences), Olympus IX-B53 inverted fluorescence microscope (Olympus Corporation), Bio-Rad 550 enzyme reader and electrophoresis/membrane transfer apparatus (both from Bio-Rad Laboratories, Inc.), and BioSpectrum 810 Imaging System (Analytik Jena AG).

Cell Counting Kit-8 (CCK-8) cell viability assay. H1299 cells in the logarithmic growth stage were divided into two groups, the DMSO and NFZ groups. The NFZ group was divided into seven sub-groups depending on the concentration of NFZ and there were three replicates in each group. The single cell suspension was aliquoted into 96-well plates, with $1x10^4$ cells/well in 100 μl DMEM, the plate was then placed in a CO_2 cell incubator at 37˚C. When the cell adhesion density reached 75%, DMEM high glucose medium containing 1% DMSO was added to the DMSO group, and DMEM high glucose medium containing 0.25, 0.5, 1, 2, 4, 8, and 16 μM NFZ was added to the NFZ sub-groups. At 24, 48 and 72 h time points, 10 μl CCK-8 solution (Yeasen Biotechnology Co., Ltd.) was added to each well and incubated in the cell incubator for 1 h, and an empty well was also filled with 10 μl CCK-8 solution as a blank group. The plate was inserted into the Bio-Rad 550 enzyme microplate reader and each group was measured at an OD of 450 nm. The experiment was repeated three times. Relative cell viability rate=[(cell experimental group A_{450}-blank group A_{450})/(cell control A_{450}-blank group A_{450})] x100%. The IC_{50} of NFZ was calculated using GraphPad Prism 8.0 software (Dotmatics).

H1299 cells were washed with PBS and digested with 25% trypsin-EDTA to form a single cell suspension that was added to 96-well plates. The plates were randomly divided into a DMSO, NFZ, GSK2606414 and NFZ + GSK2606414 group, and each group had three wells. At 24 h, cells in each group were treated, except the cells in the DMSO group. Cells in the NFZ group were treated with 20 μM NFZ medium, and cells in the GSK2606414 group were treated with 1 μM GSK2606414 medium. Cells in the NFZ + GSK2606414 group were treated with 1 μM GSK2606414 and 1 h later, 20 μM NFZ and 1 μM GSK2606414 were added in the form of liquid exchange. All plates were then placed in the incubator for incubation at 37˚C. At 24 h time points, 10 μl CCK-8 solution was added to each well and incubated in the cell incubator for 1 h. The plates were inserted into the Bio-Rad 550 enzyme microplate reader and each group was measured at an OD of 450 nm.

Optical microscopy. After digestion in 0.25% trypsin, H1299 cells were seeded into 24-well plates at $3x10^5$ cells/ml in each well. The cells were placed in the incubator, the morphological changes were observed and images were captured under an optical microscope after 24 h.

Inverted fluorescence microscopy. The grouping and dosing methods aforementioned were repeated and, 24 h later, 10 μl Brite 670 was added to the cells and the cells were incubated at 37˚C for 30 min in the dark. The cells were then washed twice with 1X PBS and images were captured using an inverted IX-B53 fluorescence microscope at x200 magnification. ImageJ (v1.53c) was used for data analysis.

Flow cytometry. H1299 cells were washed with PBS and digested with 25% trypsin-EDTA to form a single cell suspension that was added to 10-cm dishes for culturing. The plates were randomly divided into a DMSO, NFZ, GSK2606414 and NFZ + GSK2606414 group. At 24 h, cells in each group were treated, except the cells in the DMSO group. Cells in the NFZ group were treated with 20 μM NFZ medium, and cells in the GSK2606414 group were treated with 1 μM

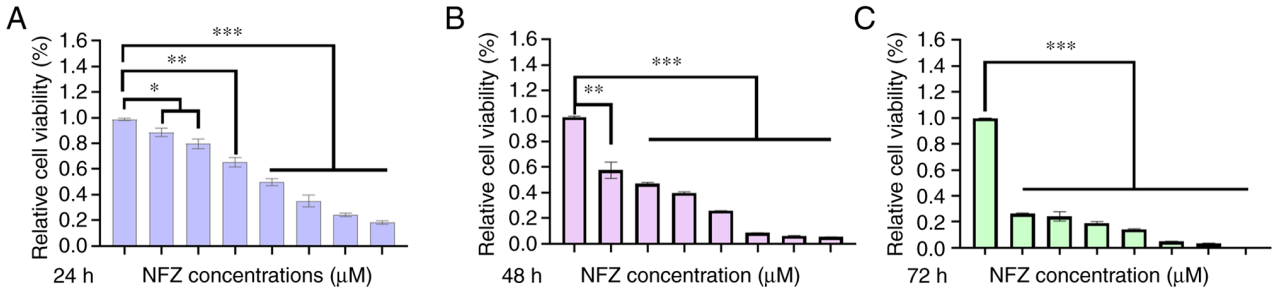

Figure 1. Effects of different concentrations of NFZ (0.25, 0.5, 1, 2, 4, 8 and 16 μM) on H1299 cell viability at (A) 24, (B) 48 and (C) 72 h. Relative cell viability was determined by Cell Counting Kit-8 assay. Compared with in the DMSO group, H1299 cell viability of even the low dose (0.25 μM) group was significantly decreased after 24 h of treatment. *P<0.05, **P<0.01, ***P<0.001. DMSO, dimethyl sulfoxide; NFZ, nifuroxazide.

GSK2606414 medium. Cells in the NFZ + GSK2606414 group were treated with 1 μM GSK2606414 and 1 h later, 20 μM NFZ and 1 μM GSK2606414 were added in the form of liquid exchange. All plates were then placed in the incubator for incubation at 37˚C for 24 h time. After treatment, the cells were digested with 0.25% trypsin and collected by centrifugation (300 x g, 4˚C, 5 min). After centrifugation, the cells were resuspended in PBS, the cell density was adjusted to 1x10^5 cells/ml and the cells were washed with PBS a further three times. For detection, 100 μl 1X binding buffer containing 5 μl Annexin V-FITC and 10 μl PI were added into each tube and incubated at 37˚C for 60 min. Subsequently, 400 μl 1X binding buffer was added to each tube for cell resuspension, and cell apoptosis was detected by BD Accuri C6 flow cytometer and the data were analyzed using FlowJo 10.0 (FlowJo LLC).

To stain intracellular ROS, 10 μl 100 μM Brite 670 was added to the treated cells and ROS was detected by flow cytometry. Brite 670 was first incubated for 30 min, and then DAPI was added for 15 min. Finally, the double-stained cells were cleaned twice with PBS, which led to observation and photography under fluorescence microscope. In addition, 200 μl Fura Red AM was added to the treated cells for intracellular Ca^{2+} staining, and the emission wavelength was detected at 550 nm. The BD Accuri C6 flow cytometer was used for detection and the data were analyzed using FlowJo 10.0 (FlowJo LLC).

Western blot analysis. After the aforementioned treatments, the cells were washed with PBS and centrifuged (300 x g, 4˚C, 5 min) to collect the suspended cells. The cells were lysed with RIPA buffer (Beyotime Institute of Biotechnology) containing 1:100 protease inhibitor and 1:100 phosphatase inhibitor, and a BCA kit was used to detect protein concentration.

Proteins (20 μg) were separated by SDS-PAGE on 10 or 12% gels. Electrophoresis and PVDF membrane transfer were performed using Bio-Rad electrophoresis and membrane transfer apparatus. For blocking, the membranes were incubated with 5% BSA (Biological Industries) on a 4˚C with agitation for 2 h. After blocking, the membranes were washed three times for 10 min intervals. Primary antibodies were added at a dilution of 1:1,000 and incubated at 4˚C overnight. Subsequently, the membranes were washed three times for 10 min intervals. After the addition of the secondary antibody at a ratio of 1:5,000, the membranes were incubated with agitation for 2 h at 4˚C and then washed three times for 10 min intervals. Finally, ECL chemiluminescence developer (Yeasen Biotechnology Co., Ltd.) was added to the membranes and, after full reaction, the membranes were placed in a Biospectrum 810 Imaging system for exposure development. The protein expression bands were observed and recorded, and the gray values of each band were analyzed by ImageJ software (v1.53c).

Statistical analysis. GraphPad Prism 8.0 software was used for statistical analysis. The data are presented as the mean ± SD. Student's t-test was used for data comparison between two unpaired groups. One-way ANOVA was applied for multiple group comparisons and Dunnett's post hoc test was performed to compare the means of multiple groups with those of a single group. All experiments were repeated three times. P<0.05 was considered to indicate a statistically significant difference.

Results

NFZ inhibits the viability of H1299 cells. After H1299 cells were treated with 0.25, 0.5, 1, 2, 4, 8 and 16 μM NFZ for 24, 48 and 72 h, the viability of the H1299 cells decreased significantly compared with that in the DMSO group and showed significant cytotoxicity, which was proportional to time and dose (Fig. 1). The IC_{50} of NFZ in H1299 cells at 24 h was calculated by GraphPad Prism 8.0. The IC_{50} in H1299 cells at 24 h was 19.78 μM; therefore, 20 μM was chosen as the experimental concentration.

NFZ induces the apoptosis of H1299 cells. H1299 cells were treated with 20 μm NFZ for 6, 12 and 24 h, and the degree of apoptosis of H1299 cells increased in a time-dependent manner. After 6 h, apoptosis began to increase significantly (Fig. 2).

NFZ increases ROS and Ca^{2+} levels in H1299 cells. After exposure to 20 μM NFZ for 24 h, compared with those in the DMSO control group, an increase in the intracellular ROS (Fig. 3A and B) and Ca^{2+} levels (Fig. 3C and D) was observed.

NFZ induces activation of the ERS-related PERK pathway. NFZ significantly increased the expression levels of P-PERK,

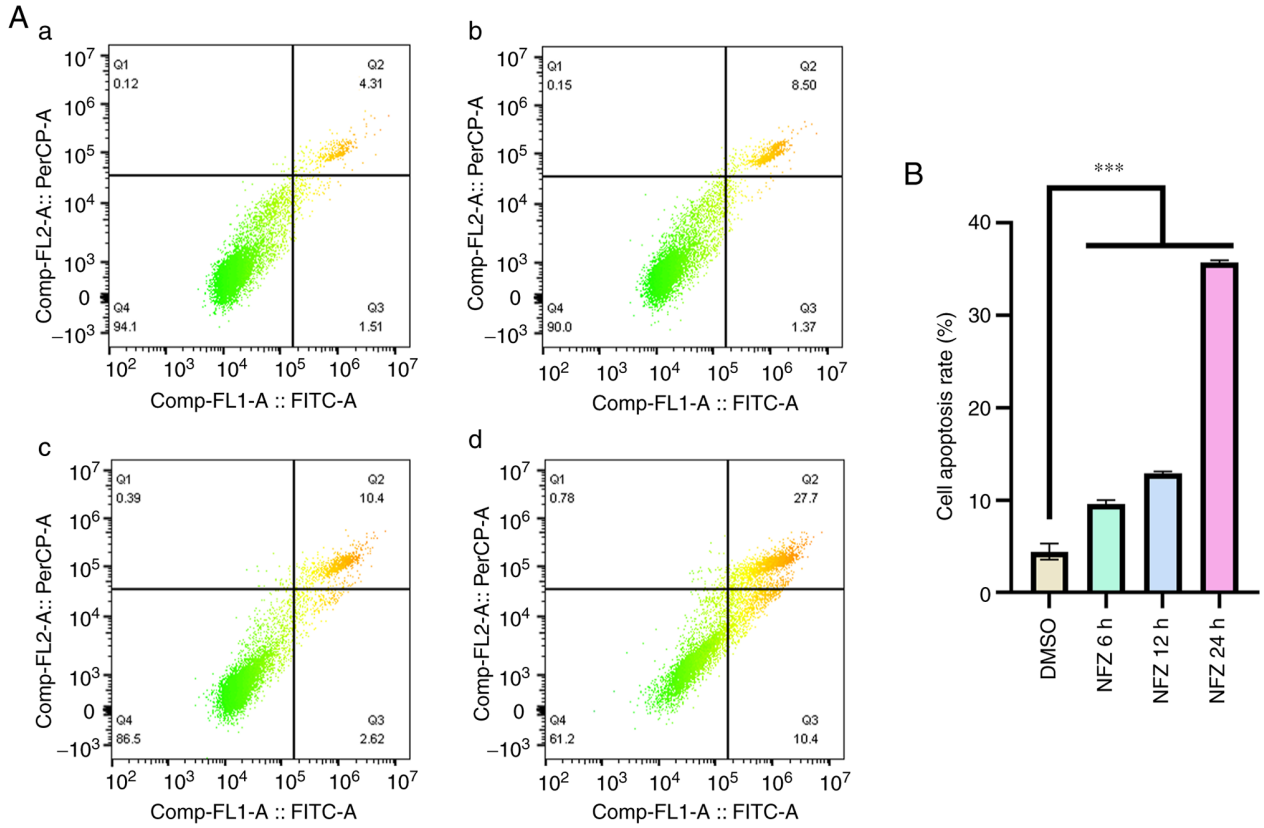

Figure 2. Apoptosis of H1299 cells induced by NFZ. H1299 cells were treated with (Aa) DMSO for 24 h, or with 20 μM NFZ for (Ab) 6, (Ac) 12 and (Ad) 24 h. Flow cytometry was used for detection. (B) Results of flow cytometric analysis. ***P<0.001. DMSO, dimethyl sulfoxide; NFZ, nifuroxazide.

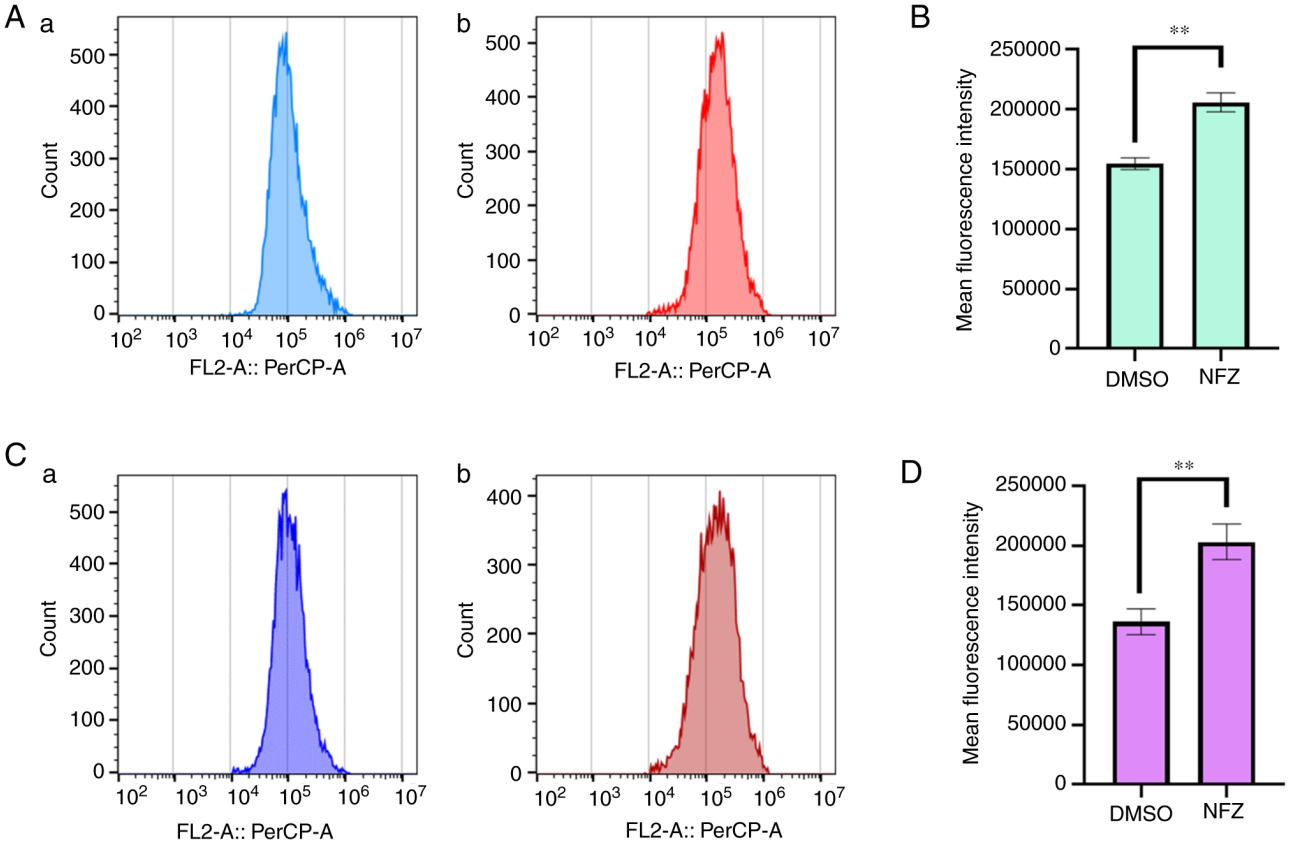

Figure 3. ROS and Ca^{2+} levels of H1299 cells treated with NFZ. ROS levels in H1299 cells after 24 h of (Aa) DMSO or (Ab) 20 μM NFZ treatment. (B) Quantification of ROS levels. Ca^{2+} levels in H1299 cells after 24 h of (Ca) DMSO or (Cb) 20 μM treatment. (D) Quantification of Ca^{2+} levels. Data are presented as the mean ± SD. **P<0.01. DMSO, dimethyl sulfoxide; NFZ, nifuroxazide; ROS, reactive oxygen species.

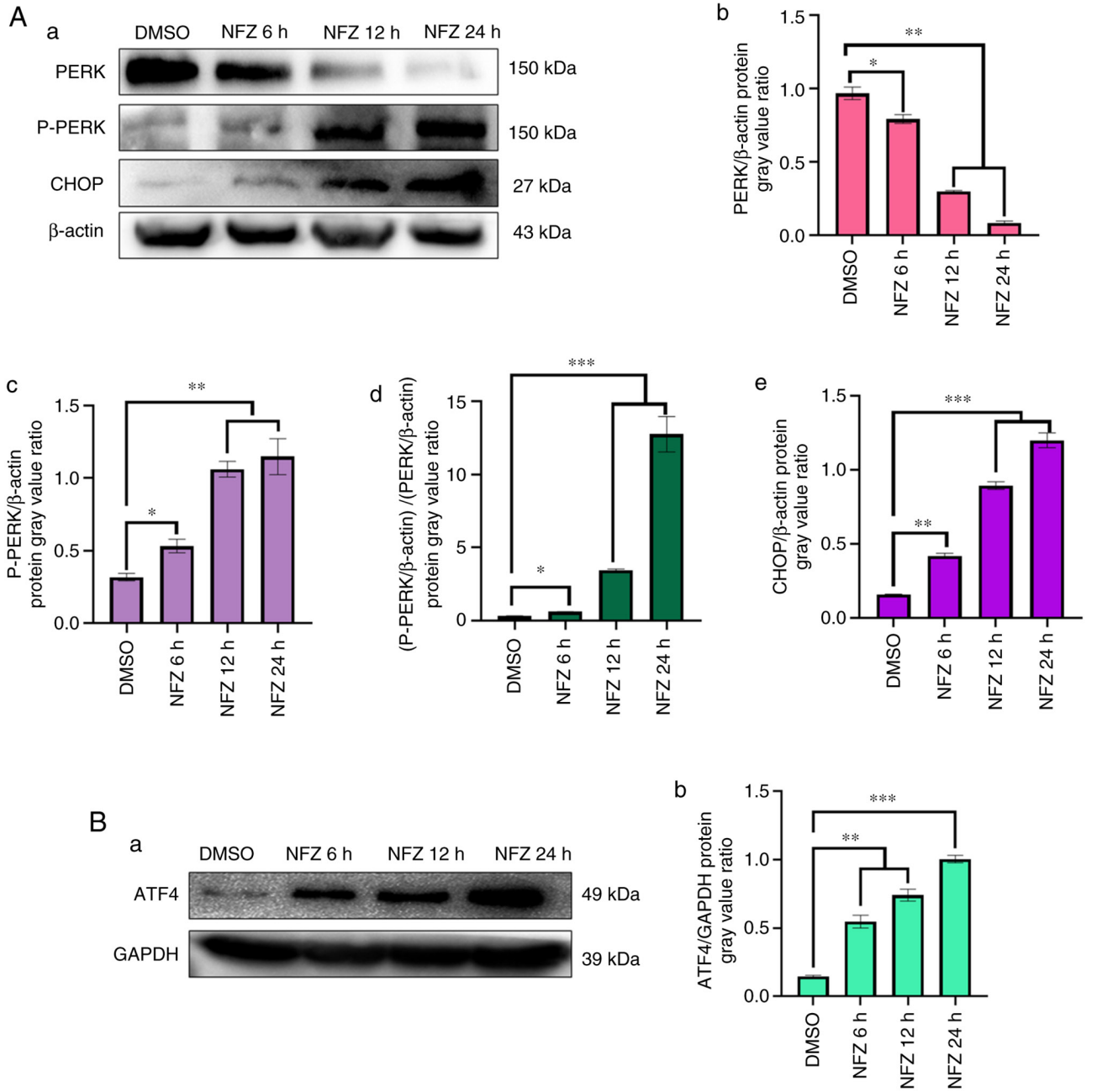

Figure 4. Changes in PERK, P-PERK, ATF4 and CHOP expression. (Aa) Expression of PERK, P-PERK and CHOP in H1299 cells exposed to NFZ for 6, 12 and 24 h. (Ab) The ratio of PERK expression relative to β-actin expression in each group. (Ac) The ratio of P-PERK expression relative to β-actin expression in each group. (Ad) The ratio of p-PERK/β-actin to PERK/β-actin. (Ae) The ratio of CHOP expression relative to β-actin expression in each group. (Ba) Expression of ATF4 in H1299 cells exposed to NFZ for 6, 12 and 24 h. (Bb) The ratio of ATF4 expression relative to GAPDH expression in each group. Data are presented as the mean ± SD. *P<0.05, **P<0.01, ***P<0.001. AFT4, activating transcription factor 4; CHOP, DNA damage inducible transcript 3; DMSO, dimethyl sulfoxide; NFZ, nifuroxazide; PERK, protein kinase R-like ER kinase.

ATF4 and CHOP, key proteins in the PERK pathway of ERS, and unphosphorylated PERK decreased with treatment of the drug, compared with that in the DMSO control group (Fig. 4). These results were observed even after 6 h of treatment.

GSK2606414 reduces the morphological changes and apoptosis induced by NFZ. Compared with in the DMSO group, the cell body of H1299 cells treated with NFZ decreased and became round, and the cells did not form colonies. A small amount of granular material appeared in the cells, there were more cell fragments in the culture medium and the cell viability was significantly decreased (Fig. 5A and B). The addition of GSK2606414 reduced the morphological changes induced by NFZ. The addition of 1 μM GSK2606414 also reduced the NFZ-induced apoptosis and cytotoxicity in H1299 cells (Fig. 5B-D).

GSK2606414 can inhibit ERS-induced by NFZ. GSK2606414 significantly reduced the increase of intracellular ROS induced by NFZ (Fig. 6). ROS is closely related to oxidative stress, and PERK is one of the classical pathways of ERS (16,17). The results of the present study indicated that

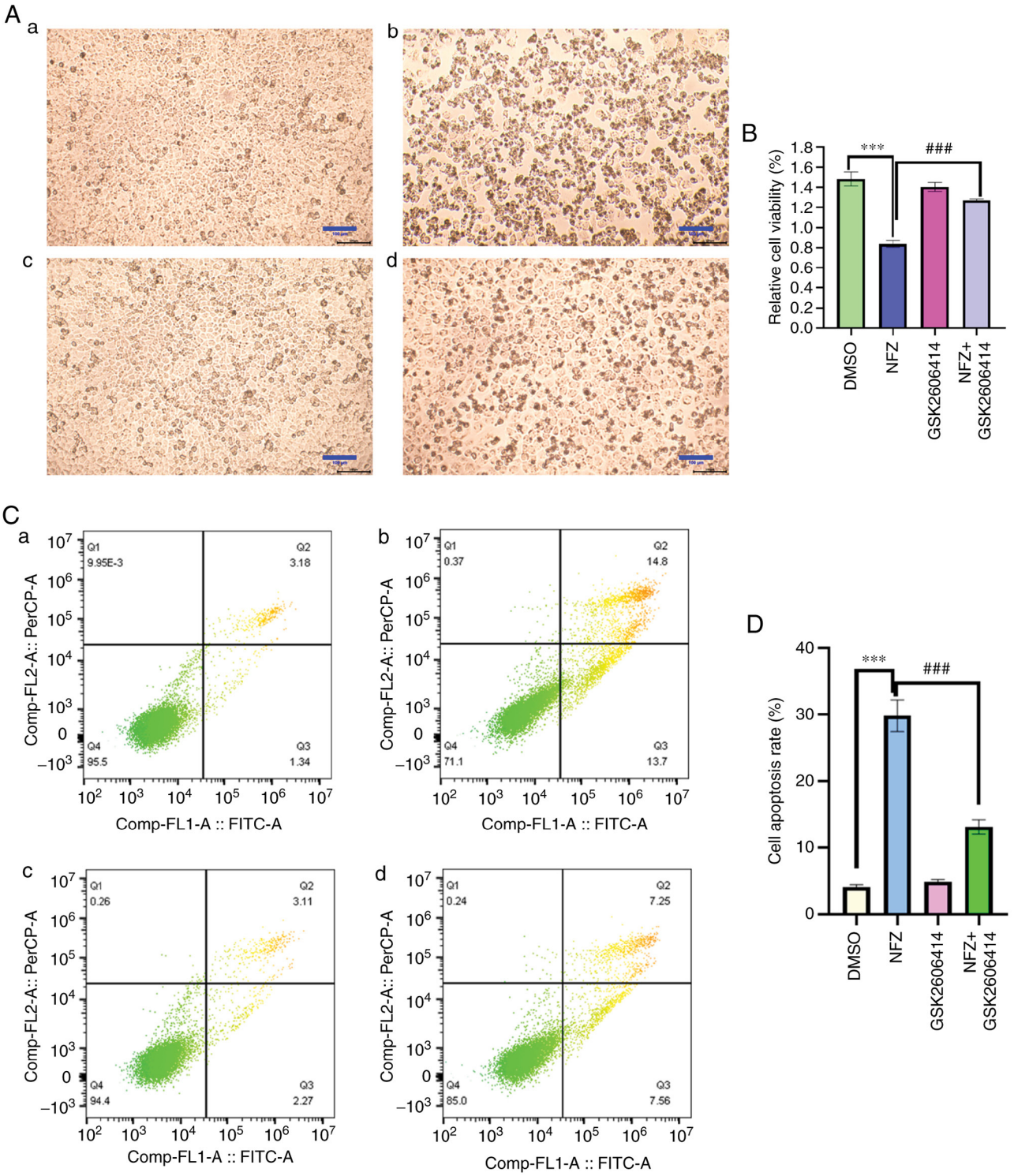

Figure 5. Effect of the protein kinase R-like ER kinase inhibitor, GSK2606414, on NFZ-induced apoptosis. Morphological changes of cells treated with NFZ for 24 h; (Aa) DMSO, (Ab) NFZ, (Ac) GSK2606414 and (Ad) NFZ + GSK2606414 groups. (B) Relative cell viability determined by Cell Counting Kit-8 assay. NFZ significantly reduced cell viability compared with the DMSO group (***P<0.001). The cytotoxicity of NFZ + GSK2606414 group was significantly lower than that of NFZ group ($^{###}$P<0.01). Apoptosis of cells treated with (Ca) DMSO, (Cb) NFZ, (Cc) GSK2606414 or (Cd) NFZ + GSK2606414. (D) Results of flow cytometric analysis. NFZ significantly reduced the cell apoptosis rate compared with the DMSO group (***P<0.001). Cell apoptosis rate induced by NFZ was significantly reduced by GSK2606414 ($^{###}$P<0.01). DMSO, dimethyl sulfoxide; NFZ, nifuroxazide.

the increase of intracellular ROS level induced by NFZ can lead to ERS. After ERS occurs, Ca^{2+} homeostasis in the ER is unbalanced and Ca^{2+} in the ER is released into the cytoplasm, which increases the level of ROS in the cytoplasm and further aggravates oxidative stress (16,17). GSK2606414 inhibited the increase in intracellular Ca^{2+} induced by NFZ (Fig. 7), indicating that Ca^{2+} release from the ER is an important mechanism of NFZ-induced H1299 cell apoptosis. GSK2606414 also inhibited the increase in P-PERK, ATF4 and CHOP protein expression levels induced by NFZ (Fig. 8).

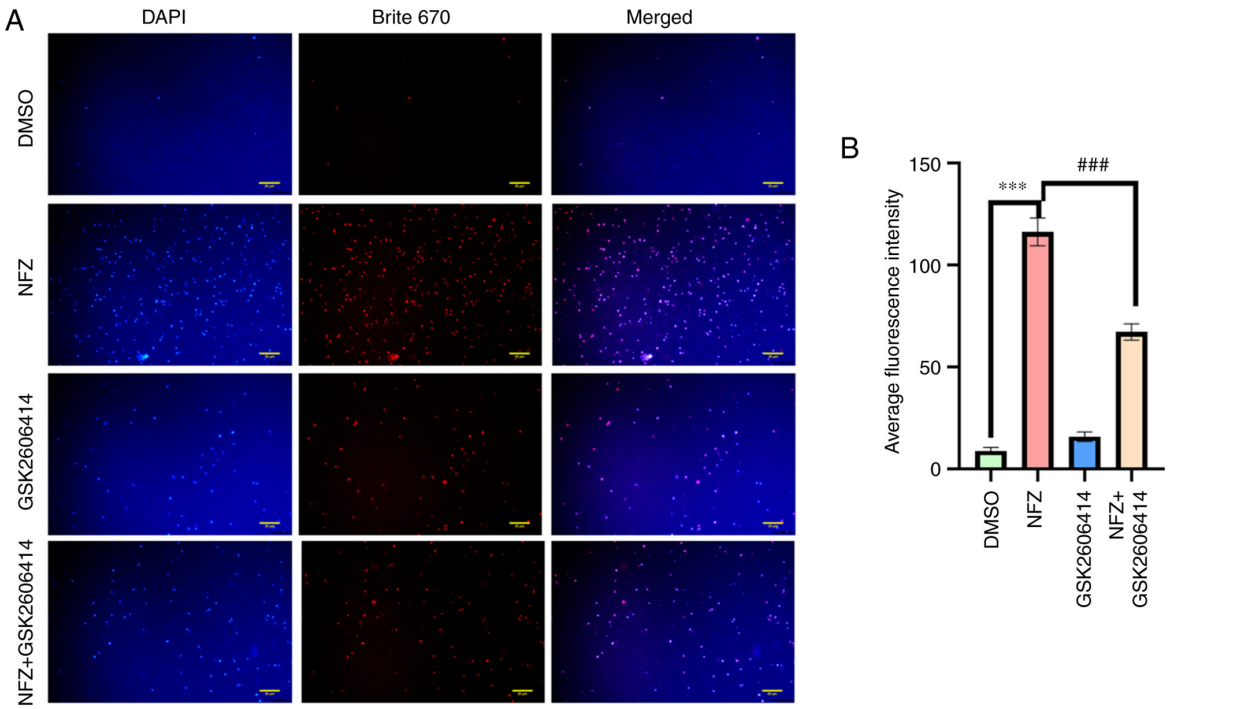

Figure 6. Effects of protein kinase R-like ER kinase inhibitor, GSK2606414, on intracellular ROS levels. (A) Levels of ROS in DMSO, NFZ, GSK2606414 and NFZ + GKS2606414 treated cells were detected by inverted fluorescence microscopy. (B) Average fluorescence intensity in each group. ***P<0.001, $^{###}$P<0.01. Scale bar, 20 μm. DMSO, dimethyl sulfoxide; NFZ, nifuroxazide; ROS, reactive oxygen species.

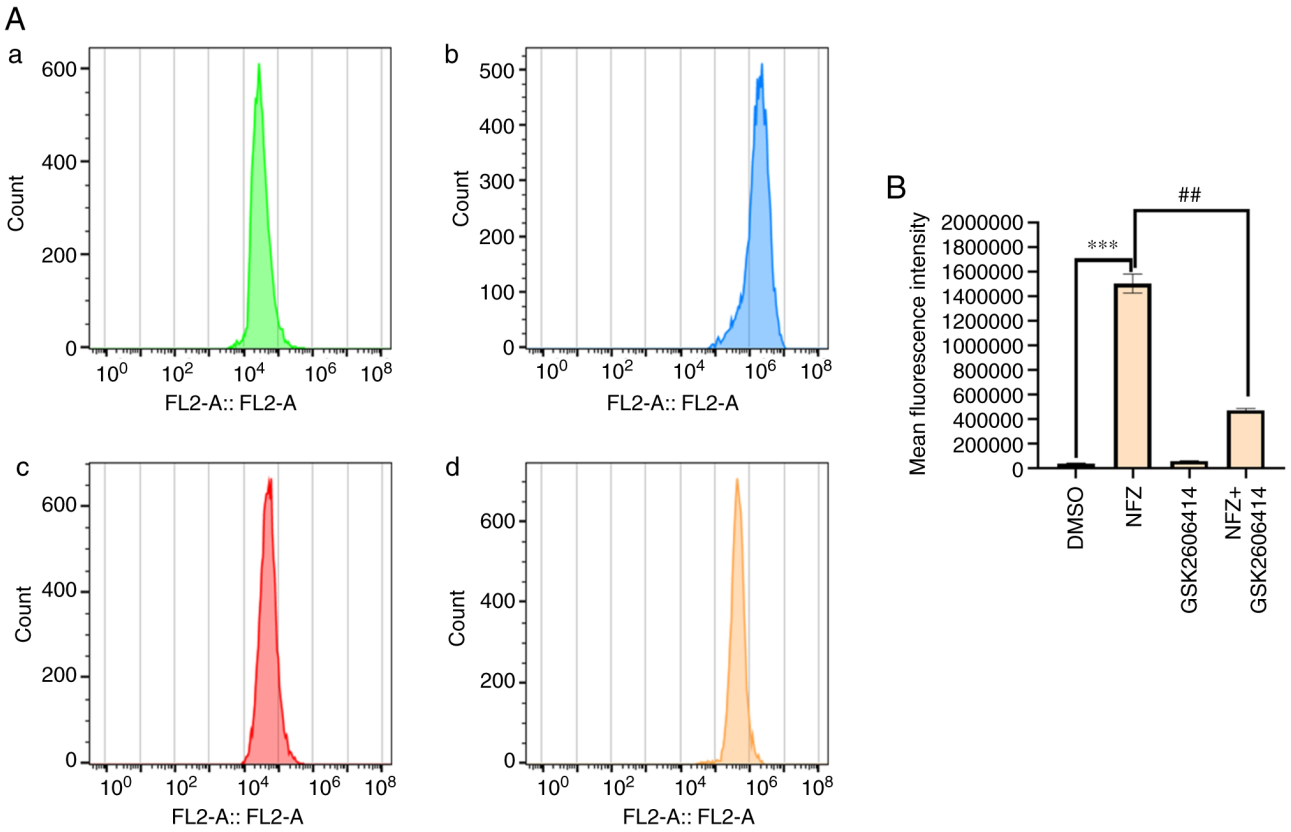

Figure 7. Changes in intracellular Ca^{2+} levels after pre-treatment with GSK2606414. (Aa) DMSO, (Ab) NFZ, (Ac) GSK2606414 and (Ad) NFZ + GSK2606414 groups. (B) Mean fluorescence intensity in each group. $^{##}$P<0.01, ***P<0.001. DMSO, dimethyl sulfoxide; NFZ, nifuroxazide.

NFZ reduces the phosphorylation of JAK2 and STAT3. The western blotting results showed that the phosphorylation levels of STAT3 and JAK2 in the NFZ group were significantly lower than those in the DMSO group. These findings

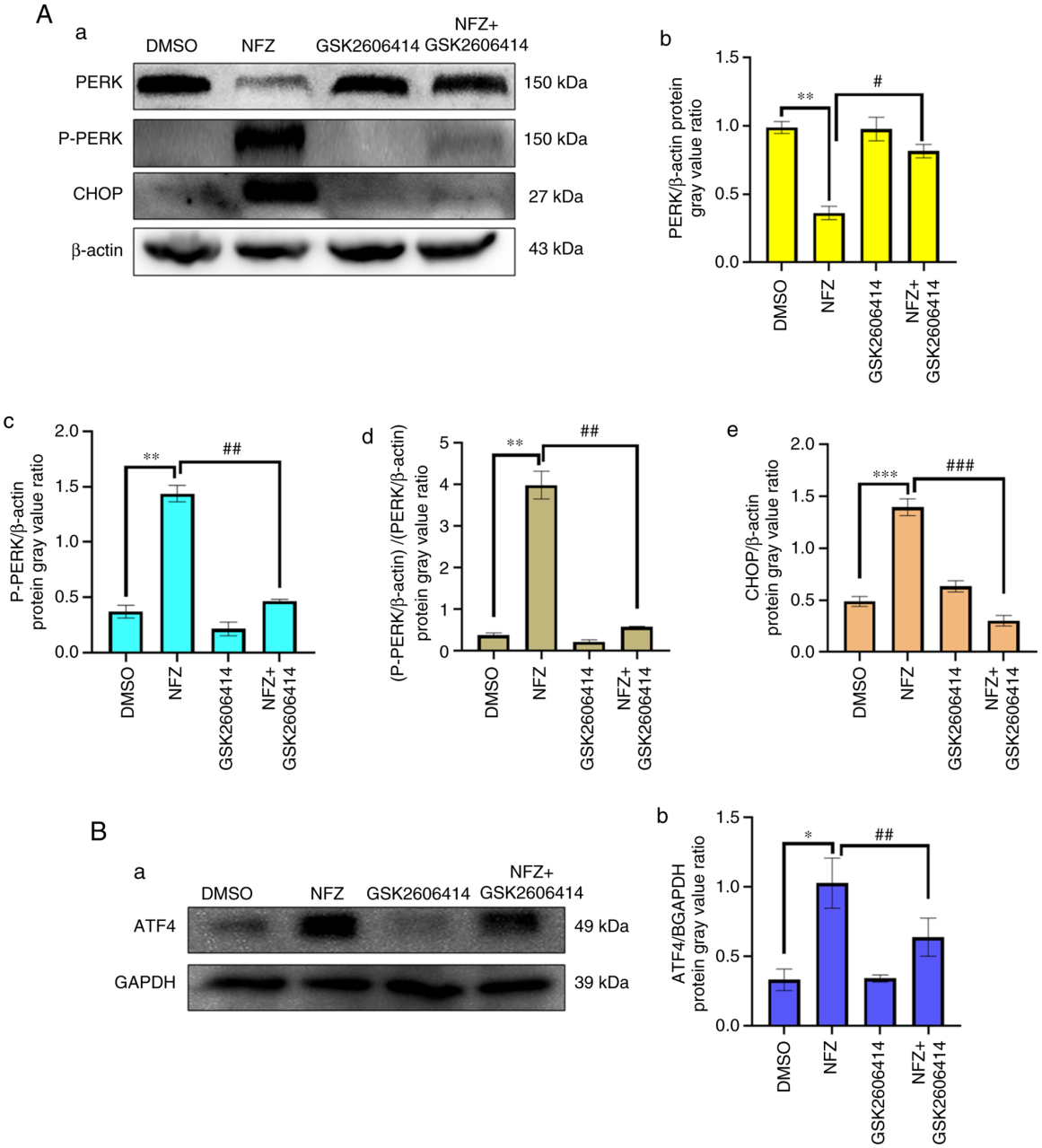

Figure 8. GSK2606414 inhibits the increases in P-PERK, ATF4 and CHOP protein expression induced by NFZ. (Aa) Changes in PERK, P-PERK, ATF4 and CHOP in DMSO, NFZ, GSK2606414 and NFZ + GSK2606414 groups. (Ab) The ratio of PERK expression relative to β-actin expression in each group. (Ac) The ratio of P-PERK expression relative to β-actin expression in each group. (Ad) The ratio of P-PERK/β-actin to PERK/β-actin. (Ae) The ratio of CHOP expression relative to β-actin expression in each group; (Ba) Expression of ATF4 in DMSO, NFZ, GSK2606414 and NFZ + GSK2606414 groups. (Bb) The ratio of ATF4 expression relative to GAPDH expression in each group. *P<0.05, **P<0.01, ***P<0.001, $^{\#}$P<0.05, $^{\#\#}$P<0.01, $^{\#\#\#}$P<0.001. AFT4, activating transcription factor 4; CHOP, DNA damage inducible transcript 3; DMSO, dimethyl sulfoxide; NFZ, nifuroxazide; PERK, protein kinase R-like ER kinase.

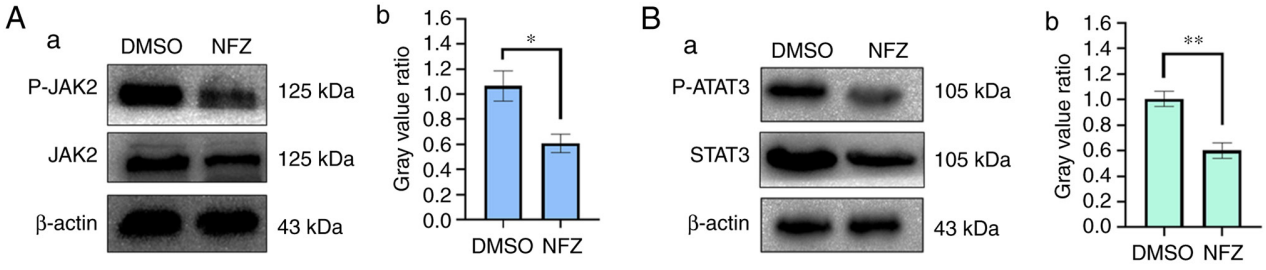

Figure 9. Changes in JAK2 and STAT3 phosphorylation after H1299 cells were exposed to NFZ for 24 h. (Aa) Expression of P-JAK2 and JAK2 in DMSO or NFZ treated groups. (Ab) Ratio of P-JAK2/β-actin to JAK2/β-actin. (Ba) Expression of P-STAT3 and STAT3 in DMSO or NFZ treated groups. (Bb) Ratio of P-JAK2/β-actin to JAK2/β-actin. *P<0.05, **P<0.01. DMSO, dimethyl sulfoxide; JAK2, Janus kinase 2; STAT3, signal transducer and activator of transcription 3; NFZ, nifuroxazide.

indicated that NFZ may be an inhibitor of JAK2 and STAT3 (Fig. 9).

Discussion

NFZ has become a research focus in recent decades due to its antitumor and JAK2 inhibitor activity (18). NFZ, an oral nitrofuran antibiotic, reduces the viability of a number of cancer cells (such as osteosarcoma, multiple myeloma, breast cancer, colorectal carcinoma and solid Ehrlich carcinoma cells) by inhibiting STAT3 phosphorylation (19-23). NFZ can significantly inhibit the migration and invasion of osteosarcoma cells through P-STAT3, MMP-2 and MMP-9 mediated signaling pathways (19). In addition, studies have shown that NFZ has antitumor cell proliferation and metastasis effects on liver cancer, breast cancer, multiple myeloma and melanoma (12,20-22,24). The occurrence of malignant tumors is due to inhibition of the apoptosis mechanism, leaving cells unable to carry out cell death and cell elimination. The induction of tumor cell apoptosis is the main way to eliminate cancer cells. Both the ER and mitochondrial pathways are typical apoptotic pathways. A previous study reported that NFZ can induce the apoptosis of osteosarcoma cells through the mitochondrial pathway (19).

Oxidative stress refers to imbalance of the redox system and the significant increase of free radicals, which exceeds the scavenging capacity of the endogenous antioxidant system (25). However, when the production of free radicals exceeds the scavenging capacity of the body, excessive ROS will accumulate in the cells and attack biological macromolecules and organelles, resulting in different degrees of oxidative stress response to DNA, proteins, lipids and carbohydrates (26). Certain studies have also demonstrated that ROS in tumor cells exceed the tolerance capacity of cells, resulting in changes in tumor cell apoptosis (27,28). The present study demonstrated that intracellular ROS were significantly increased in H1299 lung cancer cells treated with NFZ for 24 h. CCK-8 and flow cytometry experiments also demonstrated that NFZ may induce the apoptosis of H1299 cells via oxidative stress. ERS is closely related to oxidative stress and early ERS plays a cytoprotective role, but sustained ERS activates the apoptosis signaling pathway to protect the functional stability of cells (29). PERK, a member of the elF2a protein kinase family, is also a type I transmembrane protein kinase located in the ER membrane, which mainly transduces ERS signals via three typical ERS-induced apoptotic pathways involving inositol-requiring enzyme 1, PERK and ATF6 (30,31). PERK is also activated during tumor progression (32).

ERS can promote apoptosis mainly by promoting the expression of transcription factors, such as ATF4 and CHOP. ATF4 plays a key role in the transcriptional regulation of pro-survival genes mainly related to oxidative stress, autophagy, protein folding, amino acid synthesis and cell differentiation (33). The PERK signaling pathway not only reduces the folding pressure of newly synthesized proteins from the ER, but also specifically enhances the transcription level of certain genes through the fine regulatory mechanism. The upregulation of these genes is mediated by the transcription factor, ATF4 (32,34). After synthesis, ATF4 is translocated to the nucleus, and acts as a transcription factor to upregulate the transcriptional expression

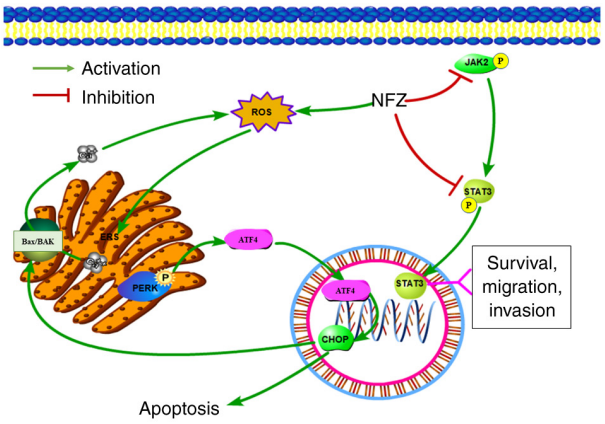

Figure 10. As a classical inhibitor of JAK2/STAT3, NFZ can induce ERS by increasing the intracellular ROS levels, thereby releasing Ca^{2+} from the ER into the cytoplasm, increasing the cytoplasmic Ca^{2+} levels and further increasing the intracellular ROS levels. In addition, the PERK pathway, the classical pathway of ERS, is activated, and the level of CHOP in the nucleus is increased, thus inducing the apoptosis of H1299 human non-small cell lung cancer cells. AFT4, activating transcription factor 4; CHOP, DNA damage inducible transcript 3; ERS, ER stress; JAK2, Janus kinase 2; NFZ, nifuroxazide; PERK, protein kinase R-like ER kinase; ROS, reactive oxygen species; STAT3, signal transducer and activator of transcription 3.

of molecular chaperones in the ER and amino acid transport proteins. However, sustained overexpression of ATF4 promotes the upregulation of the gene encoding CHOP (35,36). It has been confirmed that ERS in tumor cells leads to the activation of CHOP (32,34). Apoptosis is primarily inhibited by the presence of the anti-apoptotic molecule, Bcl-2, which has previously been observed in various tumor types (including primary cutaneous B-cell non-Hodgkin's lymphoma cells and oral squamous cells) and high expression of Bcl-2 is associated with survival and therapeutic response (37,38). A previous study reported that NFZ induces apoptosis in breast cancer through the activation of cleaved caspase-3 and Bax and the downregulation of Bcl-2 (21). Similarly, in another study, NFZ upregulated CHOP protein levels and induced the caspase molecular cascade reaction by reducing Bcl-2 levels, thus leading to apoptosis of tumor cells (39). In the present study, the experimental results demonstrated that NFZ significantly increased the expression levels of P-PERK, ATF4 and CHOP. These results indicated that NFZ may induce H1299 cell apoptosis through the PERK ERS pathway. ERS is an important pathway for cell apoptosis, and its process requires the participation of a number of molecular chaperones and specific proteins, including the transcriptional activation of CHOP and the Ca^{2+} pathway (35,40). Under ERS, Ca^{2+} is released from the ER into the cytoplasm, which causes internal Ca^{2+} overload and further aggravates ROS production, thus enhancing oxidative stress. The present study demonstrated that intracellular Ca^{2+} increased after NFZ treatment of H1299 cells for 24 h, and the PERK inhibitor, GSK2606414, significantly reduced the intracellular ROS, Ca^{2+} levels and the protein expression levels of P-PERK, ATF4 and CHOP, thus inhibiting the level of apoptosis.

As depicted in Fig. 10, NFZ may induce apoptosis of human NSCLC H1299 cells by activating the PERK-ATF4-CHOP pathway of ERS. The present study demonstrated the molecular mechanism of NFZ cytotoxicity from the perspective of

ERS-mediated apoptosis, which may provide a new basis for revealing the cytotoxicity of NFZ to tumor cells. The present study also provided some toxicological data to support the scientific and rational use of NFZ and provides a new option and molecular biological basis for the treatment of NSCLC. However, the *in vitro* culture cannot completely simulate the *in vivo* internal environment. Therefore, *in vivo* experiments will be conducted in a future study.

Acknowledgements

Not applicable.

Funding

Funding was provided by The Qingdao Applied Basic Research Program (grant no. 19-6-2-31-cg).

Availability of data and materials

The datasets generated and/or analyzed during the current study are not publicly available as the subject has not been fully concluded and the data cannot be disclosed for the time being, but are available from the corresponding author on reasonable request.

Authors' contributions

DL and LL co-wrote the manuscript. In addition, DL and LL jointly performed experiments, analyzed the experimental data and drew the pathway map. DL, LL and FL searched the literature together. FL corrected the language for some important content and helped to design some of the experiments. KG and CM designed the study together and revised the article. FL also helped to design the study. KG gave the funding support. All authors read and approved the final manuscript. All authors confirm the authenticity of all the raw data.

Ethics approval and consent to participate

Not applicable.

Patient consent for publication

Not applicable.

Competing interests

The authors declare that they have no competing interests.

References

1. Sung H, Ferlay J, Siegel RL, Laversanne M, Soerjomataram I, Jemal A and Bray F: Global Cancer Statistics 2020: GLOBOCAN estimates of incidence and mortality worldwide for 36 cancers in 185 countries. CA Cancer J Clin 71: 209-249, 2021.
2. Molina JR, Yang P, Cassivi SD, Schild SE and Adjei AA: Non-small cell lung cancer: Epidemiology, risk factors, treatment, and survivorship. Mayo Clin Proc 83: 584-594, 2008.
3. Basumallik N and Agarwal M: Small cell lung cancer. In: StatPearls [Internet]. StatPearls Publishing, Treasure Island, FL, 2022.
4. Jurisic V, Vukovic V, Obradovic J, Gulyaeva LF, Kushlinskii NE and Djordjević N: EGFR polymorphism and survival of NSCLC patients treated with TKIs: A systematic review and meta-analysis. J Oncol 2020: 1973241, 2020.
5. Jurišić V, Obradovic J, Pavlović S and Djordjevic N: Epidermal growth factor receptor gene in non-small-cell lung cancer: The importance of promoter polymorphism investigation. Anal Cell Pathol (Amst) 2018: 6192187, 2018.
6. Sharma SV, Bell DW, Settleman J and Haber DA: Epidermal growth factor receptor mutations in lung cancer. Nat Rev Cancer 7: 169-181, 2007.
7. Pushpakom S, Iorio F, Eyers PA, Escott KJ, Hopper S, Wells A, Doig A, Guilliams T, Latimer J, McNamee C, *et al*: Drug repurposing: Progress, challenges and recommendations. Nat Rev Drug Discov 18: 41-58, 2019.
8. Ward WC and Dodd MC: A comparative study of the in vitro bacteriostatic action of some simple derivatives of furan, thiophene, and pyrrole. J Bacteriol 56: 649-652, 1948.
9. Carron, MCE: Antibacterial Nitrofurfuryldene Derivatives and Methods of Using Same. US Patent US3290213A. Filed July 9, 1975; issued December 6, 1966.
10. Masunari A and Tavares LC: A new class of nifuroxazide analogues: Synthesis of 5-nitrothiophene derivatives with antimicrobial activity against multidrug-resistant Staphylococcus aureus. Bioorg Med Chem 15: 4229-4236, 2007.
11. Said E, Zaitone SA, Eldosoky M and Elsherbiny NM: Nifuroxazide, a STAT3 inhibitor, mitigates inflammatory burden and protects against diabetes-induced nephropathy in rats. Chem Biol Interact 281: 111-120, 2018.
12. Zhao T, Jia H, Cheng Q, Xiao Y, Li M, Ren W, Li C, Feng Y, Feng Z, Wang H and Zheng J: Nifuroxazide prompts antitumor immune response of TCL-loaded DC in mice with orthotopically-implanted hepatocarcinoma. Oncol Rep 37: 3405-3414, 2017.
13. Gan C, Zhang Q, Liu H, Wang G, Wang L, Li Y, Tan Z, Yin W, Yao Y, Xie Y, *et al*: Nifuroxazide ameliorates pulmonary fibrosis by blocking myofibroblast genesis: A drug repurposing study. Respir Res 23: 32, 2022.
14. Saber S, Nasr M, Kaddah MMY, Mostafa-Hedeab G, Cavalu S, Mourad AAE, Gaafar AGA, Zaghlool SS, Saleh S, Hafez MM, *et al*: Nifuroxazide-loaded cubosomes exhibit an advancement in pulmonary delivery and attenuate bleomycin-induced lung fibrosis by regulating the STAT3 and NF-κB signaling: A new challenge for unmet therapeutic needs. Biomed Pharmacother 148: 112731, 2022.
15. Liu JY, Zhang YC, Song LN, Zhang L, Yang FY, Zhu XR, Cheng ZQ, Cao X and Yang JK: Nifuroxazide ameliorates lipid and glucose metabolism in palmitate-induced HepG2 cells. RSC Adv 9: 39394-39404, 2019.
16. Caballano-Infantes E, Terron-Bautista J, Beltrán-Povea A, Cahuana GM, Soria B, Nabil H, Bedoya FJ and Tejedo JR: Regulation of mitochondrial function and endoplasmic reticulum stress by nitric oxide in pluripotent stem cells. World J Stem Cells 9: 26-36, 2017.
17. Cao S, Tang J, Huang Y, Li G, Li Z, Cai W, Yuan Y, Liu J, Huang X and Zhang H: The road of solid tumor survival: From drug-induced endoplasmic reticulum stress to drug resistance. Front Mol Biosci 8: 620514, 2021.
18. da Costa MOL, Pavani TFA, Lima AN, Scott AL, Ramos DFV, Lazarini M and Rando DGG: Nifuroxazide as JAK2 inhibitor: A binding mode proposal and Hel cell proliferation assay. Eur J Pharm Sci 162: 105822, 2021.
19. Luo Y, Zeng A, Fang A, Song L, Fan C, Zeng C, Ye T, Chen H, Tu C and Xie Y: Nifuroxazide induces apoptosis, inhibits cell migration and invasion in osteosarcoma. Invest New Drugs 37: 1006-1013, 2019.
20. Nelson EA, Walker SR, Kepich A, Gashin LB, Hideshima T, Ikeda H, Chauhan D, Anderson KC and Frank DA: Nifuroxazide inhibits survival of multiple myeloma cells by directly inhibiting STAT3. Blood 112: 5095-5102, 2008.
21. Yang F, Hu M, Lei Q, Xia Y, Zhu Y, Song X, Li Y, Jie H, Liu C, Xiong Y, *et al*: Nifuroxazide induces apoptosis and impairs pulmonary metastasis in breast cancer model. Cell Death Dis 6: e1701, 2015.
22. Ye TH, Yang FF, Zhu YX, Li YL, Lei Q, Song XJ, Xia Y, Xiong Y, Zhang LD, Wang NY, *et al*: Inhibition of Stat3 signaling pathway by nifuroxazide improves antitumor immunity and impairs colorectal carcinoma metastasis. Cell Death Dis 8: e2534, 2017.

23. El-Sherbiny M, El-Sayed RM, Helal MA, Ibrahiem AT, Elmahdi HS, Eladl MA, Bilay SE, Alshahrani AM, Tawfik MK, Hamed ZE, *et al*: Nifuroxazide mitigates angiogenesis in Ehlrich's solid carcinoma: Molecular docking, bioinformatic and experimental studies on inhibition of Il-6/Jak2/Stat3 signaling. Molecules 26: 6858, 2021.
24. Zhu Y, Ye T, Yu X, Lei Q, Yang F, Xia Y, Song X, Liu L, Deng H, Gao T, *et al*: Nifuroxazide exerts potent anti-tumor and anti-metastasis activity in melanoma. Sci Rep 6: 20253, 2016.
25. Schieber M and Chandel NS: ROS function in redox signaling and oxidative stress. Curr Biol 24: R453-R462, 2014.
26. Sies H: Oxidative stress: Oxidants and antioxidants. Exp Physiol 82: 291-295, 1997.
27. Liu L, Sun X, Guo Y and Ge K: Evodiamine induces ROS-Dependent cytotoxicity in human gastric cancer cells via TRPV1/Ca^{2+} pathway. Chem Biol Interact 351: 109756, 2022.
28. Sun Y, St Clair DK, Xu Y, Crooks PA and St Clair WH: A NADPH oxidase-dependent redox signaling pathway mediates the selective radiosensitization effect of parthenolide in prostate cancer cells. Cancer Res 70: 2880-2890, 2010.
29. Xiao B, Liu C, Liu BT, Zhang X, Liu RR and Zhang XW: TTF1-NPs Induce ERS-Mediated apoptosis and inhibit human hepatoma cell growth in vitro and in vivo. Oncol Res 23: 311-320, 2016.
30. Limia CM, Sauzay C, Urra H, Hetz C, Chevet E and Avril T: Emerging roles of the endoplasmic reticulum associated unfolded protein response in cancer cell migration and invasion. Cancers (Basel) 11: 631, 2019.
31. Oakes SA: Endoplasmic reticulum stress signaling in cancer cells. Am J Pathol 190: 934-946, 2020.
32. Rozpedek W, Pytel D, Mucha B, Leszczynska H, Diehl JA and Majsterek I: The role of the PERK/eIF2α/ATF4/CHOP signaling pathway in tumor progression during endoplasmic reticulum stress. Curr Mol Med 16: 533-544, 2016.
33. Chen D, Fan Z, Rauh M, Buchfelder M, Eyupoglu IY and Savaskan N: ATF4 promotes angiogenesis and neuronal cell death and confers ferroptosis in a xCT-dependent manner. Oncogene 36: 5593-5608, 2017.
34. Kania E, Pająk B and Orzechowski A: Calcium homeostasis and ER stress in control of autophagy in cancer cells. Biomed Res Int 2015: 352794, 2015.
35. Oyadomri S and Mori M: Roles of CHOP/GADD153 in endoplasmic reticulum stress. Cell Death Differ 11: 381-389, 2004.
36. Guo FJ, Liu Y, Zhou J, Luo S, Zhao W, Li X and Liu C: XBP1S protects cells from ER stress-induced apoptosis through Erk1/2 signaling pathway involving CHOP. Histochem Cell Biol 138: 447-460, 2012.
37. Colovic N, Jurisic V, Terzic T, Atkinson HD and Colovic M: Immunochemotherapy for Bcl-2 and MUM-negative aggressive primary cutaneous B-cell non-Hodgkin's lymphoma. Arch Dermatol Res 301: 689-692, 2009.
38. Popović B, Jekić B, Novaković I, Luković LJ, Tepavcević Z, Jurisić V, Vukadinović M and Milasin J: Bcl-2 expression in oral squamous cell carcinoma. Ann N Y Acad Sci 1095: 19-25, 2007.
39. Karan-Djurasevic T, Palibrk V, Zukic B, Spasovski V, Glumac I, Colovic M, Colovic N, Jurisic V, Scorilas A, Pavlovic S and Tosic N: Expression of Bcl2L12 in chronic lymphocytic leukemia patients: Association with clinical and molecular prognostic markers. Med Oncol 30: 405, 2013.
40. Xiao B, Lin D, Zhang X, Zhang M and Zhang X: TTF1, in the form of nanoparticles, inhibits angiogenesis, cell migration and cell invasion in vitro and in vivo in human hepatoma through STAT3 regulation. Molecules 21: 1507, 2016.